

# Improved Frequency Response of Microstrip Lowpass Filter Using Defected Ground Structures

Thulaseedharan K. Rekha<sup>1, \*</sup>, Parambil Abdulla<sup>1</sup>,  
Puthenveetil M. Jasmine<sup>2</sup>, and Paruthikkal M. Raphika<sup>2</sup>

**Abstract**—The frequency response characteristics of a basic microstrip lowpass filter improved using H-shaped defected ground structures are presented. The proposed defected ground structures behave as a resonant element at high frequency and thus eliminate the stopband frequencies to achieve wide stopband rejection. The 3 dB cutoff frequency of the filter is 1.935 GHz. Due to the defects etched in the ground plane of the basic structure, the harmonic rejection is improved from 5th to 10th order along with low insertion loss and voltage standing wave ratio together with good selectivity. The compact filter has a size of  $0.0338\lambda_g^2$ , with  $\lambda_g = 85.18$  mm being the guided wavelength at the cutoff frequency. The characteristics of the lowpass filter are verified through simulation and measurement. Consistent and stable results are obtained.

## 1. INTRODUCTION

Lowpass filters are vital components in microwave and wireless communication devices. Compactness, unity voltage standing wave ratio, low insertion loss, high degree of harmonic rejection and good selectivity are the most desirable parameters in the design of lowpass filters. Conventional microstrip lowpass filter designs using stepped impedance resonators and uniform impedance stubs have only limited harmonic rejection in the stopband [1, 2]. To extend the stopband bandwidth, additional attenuation poles have to be added, which will increase the size of the filter [3]. In [4], wide stopband suppression level and improved impedance matching are achieved by the introduction of symmetrically loaded resonant patches, open stubs and a stair-shaped high impedance stub. A compact lowpass filter with sharp roll-off is achieved using a coupled line hairpin unit in [5]. Recently, defected ground structures (DGSs) realized by etching a few defects in the ground plane have been a subject of increasing interest in analyzing the microstrip line characteristics, and the size, shape and orientation of the slot have significant influence on the performance of the lowpass filter [6–9]. However, the stopband of these filters is not wide enough to remove the undesired harmonics. Cascades of inductively coupled fractal defected ground resonators are utilized in [10] to design a microstrip lowpass filter with high stopband suppression level. In [11], a compact lowpass filter is designed using quasi-Yagi DGS resonators to improve the stopband and to reduce the losses. To improve the roll-off rate of the filter, the DGS cells combined with stepped impedance resonators are presented in [12, 13]. Using a complementary rectangle split ring defected microstrip structure (CRSR-DMS) and DGSs, a lowpass filter with good passband and wide stopband performance is designed in [14]. A high performance lowpass filter suitable for microwave mixer application is introduced in [15] and has good characteristics such as sharp selectivity and wide stopband. In [16] a meandered slot resonator is designed to develop a compact lowpass

---

Received 20 November 2017, Accepted 24 January 2018, Scheduled 30 January 2018

\* Corresponding author: Thulaseedharan Kodiyattuvila Rekha (rekhamuralitk@gmail.com).

<sup>1</sup> School of Engineering, Cochin University of Science and Technology, Cochin, Kerala, India. <sup>2</sup> M.E.S. College Marampally, Aluva, Kerala, India.

filter with a uniform transmission line. However, compactness, passband return loss and suppression of harmonics in the stopband have to be improved further in most of these filters.

In this paper, a basic microstrip lowpass filter is designed using stepped impedance resonators and uniform impedance stubs (SIR-UIS). The designed filter has a stopband bandwidth up to 9.874 GHz at 20 dB suppression level. The performance of the basic filter is improved using H-shaped DGS resonators etched on the surface of the metallic ground plane. The DGS resonators improve the selectivity of the filter together with a wide stopband at 20 dB rejection level. The proposed DGS filters have better performance than most of the previously mentioned DGS lowpass filters, as far as the frequency response and size reduction are concerned.

## 2. BASIC MICROSTRIP LOWPASS FILTER DESIGN

Conventional lowpass filter design using SIR-UIS has the capability to generate transmission zeros at their resonant frequencies [2]. To obtain a wider stopband, more elements have to be added which will naturally increase the physical size of the filter. Here, a basic microstrip lowpass filter is designed using SIR-UIS to achieve the desired characteristics.

Before going into the basic filter design, a primary resonator is analyzed. A series resonant branch having a high impedance stub and a low impedance patch, modeled as inductor and capacitor respectively [2], is connected in shunt with a high impedance main transmission line as shown in Figure 1(a). The dimensions are  $l'_1 = 6.4$  mm,  $l'_2 = 4$  mm,  $l'_3 = 3.6$  mm,  $w' = 0.2$  mm and  $w'_1 = 3.6$  mm. The high impedance main transmission line of length  $l'_1$  is represented as  $Z_{L1}$  and the impedance of the series resonant branches are  $Z_{L2}$  and  $Z_{C1}$  respectively. The width,  $w'_o$ , of the microstrip line is chosen to be 1.5 mm which corresponds to the characteristic impedance of  $50 \Omega$ . All simulations are carried out using full wave EM simulator IE3D and the substrate used is FR4 with relative dielectric constant 4.4, thickness  $h = 0.8$  mm and dielectric loss tangent 0.02. The  $LC$  equivalent circuit of the primary resonator is shown in Figure 1(b). The values of  $L$  and  $C$  are calculated using [2].  $L'_1 = 4.437$  nH,  $L'_2 = 3.273$  nH and  $C'_1 = 0.9108$  pF.

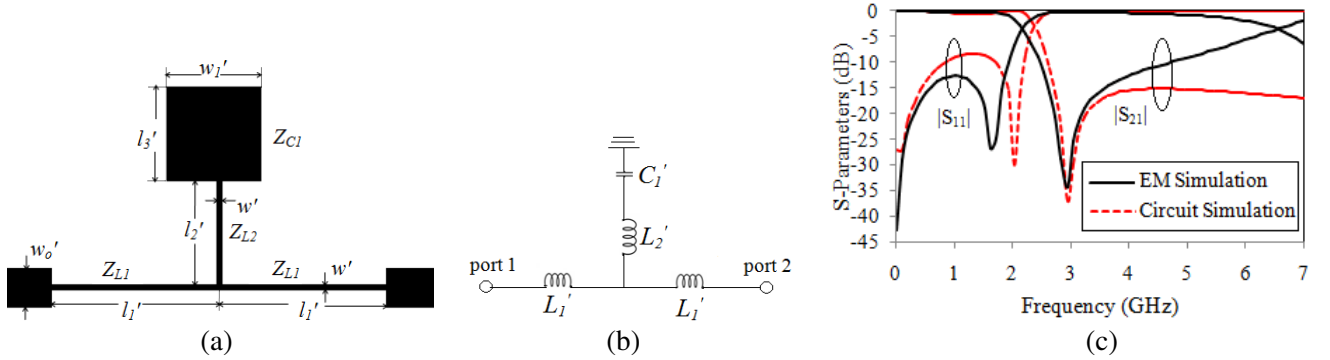


**Figure 1.** The primary resonator. (a) Structure. (b) LC equivalent circuit. (c) Frequency response characteristics.

The  $ABCD$  parameters of the symmetrical two-port T-network [1], shown in Figure 1(a), are

$$A = D = 1 + \frac{Z_{L1}}{Z_{L2} + Z_{C1}} \quad (1)$$

$$B = 2(Z_{L1}) + \frac{Z_{L1}^2}{Z_{L2} + Z_{C1}} \quad (2)$$

$$C = \frac{1}{Z_{L2} + Z_{C1}} \quad (3)$$

Substituting the impedance of the inductors and capacitor,

$$A = D = 1 + \frac{\omega^2 L'_1 C'_1}{\omega^2 L'_2 C'_1 - 1} \quad (4)$$

$$B = \frac{2j\omega L'_1 - 2j\omega^3 L'_1 L'_2 C'_1 - j\omega^3 (L'_1)^2 C'_1}{1 - \omega^2 L'_2 C'_1} \quad (5)$$

$$C = \frac{j\omega C'_1}{1 - \omega^2 L'_2 C'_1} \quad (6)$$

The  $S$ -parameters of the primary resonator [1] are,

$$S_{11} = \frac{A + B/Z_0 - CZ_0 - D}{A + B/Z_0 + CZ_0 + D} \quad S_{21} = \frac{2}{A + B/Z_0 + CZ_0 + D} \quad (7)$$

Substituting Eqs. (4)–(6) in Equation (7),

$$S_{11} = \frac{2j\omega L'_1 (1 - \omega^2 L'_2 C'_1) - j\omega C'_1 (\omega^2 (L'_1)^2 + Z_0^2)}{2Z_0 (1 - \omega^2 L'_2 C'_1 - \omega^2 L'_1 C'_1) + 2j\omega L'_1 (1 - \omega^2 L'_2 C'_1) - j\omega C'_1 (\omega^2 (L'_1)^2 - Z_0^2)} \quad (8)$$

$$S_{21} = \frac{2Z_0 (1 - \omega^2 L'_2 C'_1)}{2Z_0 (1 - \omega^2 L'_2 C'_1 - \omega^2 L'_1 C'_1) + 2j\omega L'_1 (1 - \omega^2 L'_2 C'_1) - j\omega C'_1 (\omega^2 (L'_1)^2 - Z_0^2)} \quad (9)$$

From Eqs. (8)–(9) it is clear that the transmission and reflection characteristics are controlled by varying the values of  $L'_1$ ,  $L'_2$  and  $C'_1$ . By setting  $|S_{21}| = 0$ , a single finite frequency attenuation pole occurs at  $f_p$  and is given in Equation (10).

$$f_p = \frac{1}{2\pi\sqrt{L'_2 C'_1}} \quad (10)$$

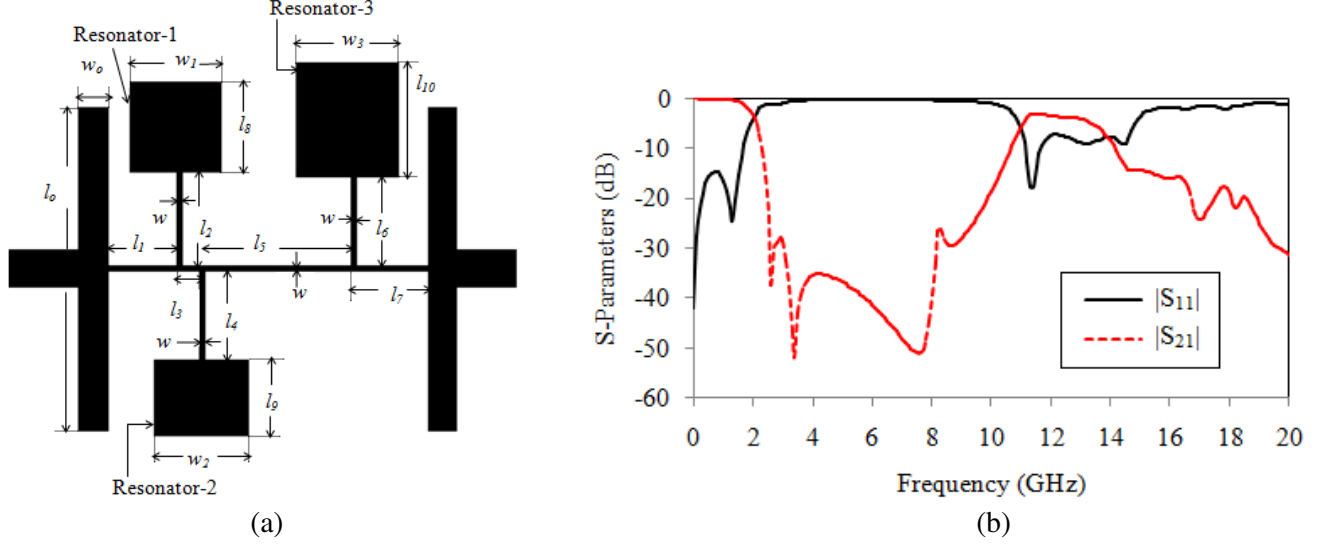
The calculated value of resonant frequency  $f_p$  is 2.914 GHz.

Figure 1(c) shows the simulated frequency responses of the EM and LC circuit of the primary resonator, and both results are in good agreement with theory. The cutoff frequency of the microstrip implementation of the structure is 2.13 GHz, and the single transmission zero occurs at 2.916 GHz.

By using the same idea, the primary resonator is extended to the basic microstrip lowpass filter design using SIR-UIS to obtain a wide stopband up to 9.874 GHz at 20 dB suppression level, shown in Figure 2(a). The structure consists of two uniformly shaped low impedance stubs and three stepped impedance resonators, Resonator-1, Resonator-2 and Resonator-3 loaded on the high impedance main transmission line. The uniformly shaped low impedance stubs can be modeled as a capacitor, having width and length  $l_o$  and  $w_o$  respectively. The three stepped impedance resonators have a high impedance line loaded by low impedance square and rectangular patches as represented in Figure 2(a). The dimensions of the layout are  $w = 0.2$ ,  $w_1 = 3.6$ ,  $w_2 = 3.7$ ,  $w_3 = 4.05$ ,  $w_o = 1.15$ ,  $l_1 = 2.8$ ,  $l_2 = 3.8$ ,  $l_3 = 0.9$ ,  $l_4 = 3.6$ ,  $l_5 = 6.05$ ,  $l_6 = 3.6$ ,  $l_7 = 3.05$ ,  $l_8 = 3.6$ ,  $l_9 = 3.0$ ,  $l_{10} = 4.55$ ,  $l_o = 13.0$  (all in mm). The frequency response of the basic lowpass filter is shown in Figure 2(b). The cutoff frequency of the filter is 1.95 GHz, and the frequency at 20 dB suppression level is 2.464 GHz. The selectivity of the filter is 33.36 dB/GHz. The insertion loss is less than 0.35 dB up to 1.1 GHz of the passband, and the return loss in the passband is better than 14.7 dB. The stopband bandwidth at 20 dB suppression level is from 2.464 GHz to 9.874 GHz, and the relative stopband bandwidth (RSB) calculated as a percentage (the ratio of stopband bandwidth to stopband centre frequency) is 120.1%. The physical size of the filter is only 15.1 mm  $\times$  14.95 mm.

The main drawback of this filter is the presence of out of band spurious frequencies. To improve the performance, these components have to be suppressed, without increasing the physical size. DGS is an appropriate choice due to its attractive features such as simplicity, wide and deeper stopband characteristics.

To improve the performance of the basic lowpass filter without compromising the size, defected ground structures are used to design the proposed filter, Filter-1. It is the same SIR-UIS structure with two symmetrical H-shaped slots etched on the ground plane. The size and shape of DGS are selected such that it should resonate at a higher frequency so as to extend the stopband bandwidth of the basic structure.



**Figure 2.** (a) Layout of the basic lowpass filter. (b) Simulated frequency response.

### 3. CHARACTERISTICS OF H-SHAPED DGS

A one-pole microstrip lowpass filter with an H-shaped slot etched on the metallic ground plane is analyzed, and its structure is shown in Figure 3(a). In order to analyze the frequency characteristics of the DGS section, the structure is simulated with IE3D software. The dimensions of the DGS unit shown in Figure 3(a) are  $a = 7.1$  mm,  $b = 1.6$  mm,  $c = 1.8$  mm,  $d = 2.2$  mm and  $w'_o = 1.5$  mm. The EM simulated transmission response of Figure 3(a) is in Figure 3(b), and this unit DGS section can provide the desired cutoff and attenuation pole frequency values. The cutoff frequency of the filter is 10.26 GHz, and the transmission zero occurs at 14.85 GHz. As seen in Figure 3(b), wide stopband bandwidth is achieved by using the H-shaped DGS. The equivalent circuit of the H-shaped DGS can be modeled as a parallel LC circuit as shown in Figure 3(c). Depending on the size and shape of the etched lattice, an attenuation pole can be generated by the combination of inductance and capacitance elements. By employing the proposed etched lattice, the effective permittivity and thereby the reactance of the microstrip line are increased. The values of  $L$  and  $C$  can be derived by using the EM simulation result. The reactance value of the proposed DGS section can be expressed using [6] as

$$X_{LC} = \frac{1}{\omega_o C_H \left( \frac{\omega_o}{\omega} - \frac{\omega}{\omega_o} \right)} \quad (11)$$

where  $\omega_o$  is the angular resonance frequency at 14.85 GHz. The series inductance  $X_L$  of Butterworth lowpass filter can be derived by using [2] as

$$X_L = \omega L = \frac{\omega}{\omega_c} (Z_0 g_1) \quad (12)$$

where  $\omega_c$  is the angular 3 dB cutoff frequency,  $Z_0$  the source impedance, and  $g_1$  the prototype element value of Butterworth lowpass filter. The circuit parameters of Figure 3(c) are calculated by equating the reactance values of the DGS structure and one pole Butterworth lowpass filter at the cutoff frequency and thus the capacitance  $C_H$  and the inductance  $L_H$  can be calculated by using Equations (13)–(15).

$$\frac{1}{\omega_o C_H \left( \frac{\omega_o}{\omega_c} - \frac{\omega_c}{\omega_o} \right)} = Z_0 g_1 \quad (13)$$

$$C_H = \frac{\omega_c}{Z_0 g_1 (\omega_o^2 - \omega_c^2)} \quad (14)$$

$$L_H = \frac{1}{4\pi^2 f_o^2 C_H} \quad (15)$$

The discontinuity of the DGS structure in the ground plane results in large fringing fields, and it can be represented by the capacitance  $C_p$ . The capacitance  $C_p$  changes the value of characteristic impedance and its value is calculated using [7]. The calculated values of equivalent lumped elements of Figure 3(c) are  $L_H = 0.8089$  nH,  $C_H = 0.142$  pF, and  $C_p = 0.28$  pF. The simulated EM and LC equivalent circuit results are shown in Figure 3(b). The current distribution of one pole H-shaped DGS at the resonant frequency is shown in Figure 3(d). The transmitted energy is reflected back to the source, and thus the transmission zero occurs at the resonant frequency of 14.85 GHz.

The increase in parameter  $a$  causes a corresponding increase in effective inductance of the etched

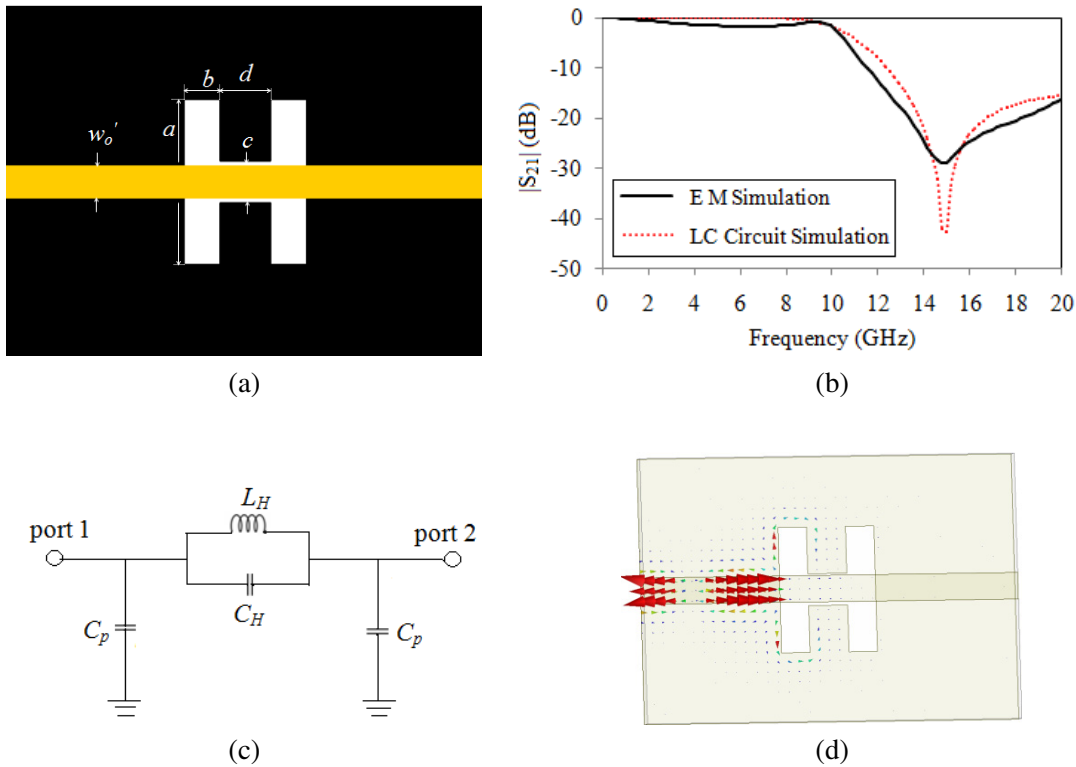


**Figure 3.** One pole H-shaped DGS lowpass filter. (a) Schematic diagram, (b) transmission response of EM and LC circuit simulation, (c) LC equivalent circuit, and (d) current distribution at resonant frequency.

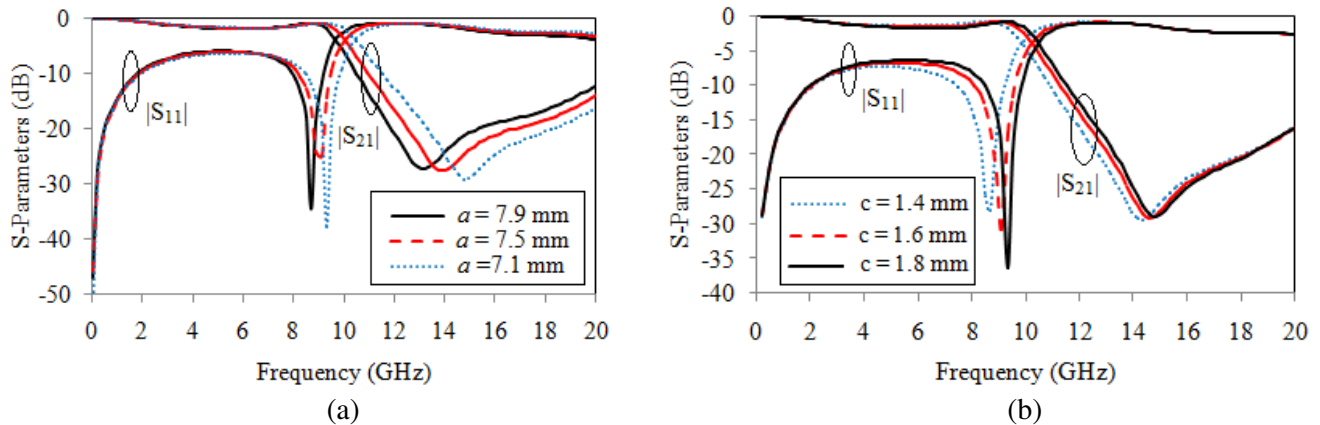


**Figure 4.** Frequency response of H-shaped DGS (a) for various values of  $a$ , (b) for various values of  $c$ .

structure which results in lowering the cutoff frequency as depicted in Figure 4(a). For the selected value of  $a = 7.1$  mm, the suppression level is found to increase. As the value of  $c$  increases from 1.4 mm to 1.8 mm, the effective capacitance of the etched lattice decreases, and the resonance frequency is found to increase as shown in Figure 4(b).

#### 4. COMPACT STEPPED IMPEDANCE LOWPASS FILTER WITH WIDE STOPBAND

Figures 5(a) and 5(b) show the top and bottom views of the proposed lowpass filter, named as Filter-1, which consists of two symmetric H-shaped DGSs etched on the ground metallic plane of the basic lowpass filter structure. Two H-shaped units in the ground plane are separated by the spacing,  $s = 4.1$  mm. The stopband bandwidth of the filter is improved by the use of etched units in the ground plane without increasing the physical size. The introduced H-shaped DGS units allow good selectivity and wide stopband bandwidth up to 20 GHz at 18 dB suppression level. The simulated 3 dB cutoff frequency of Filter-1 is 1.945 GHz, and wide stopband bandwidth from 2.315 GHz to 20 GHz with rejection level of 18 dB is achieved. The selectivity of the filter is 42.71 dB/GHz at 20 dB suppression level. The insertion loss is lower than 0.3 dB up to 1.1 GHz of the passband, and the return loss is higher than 30.4 dB.

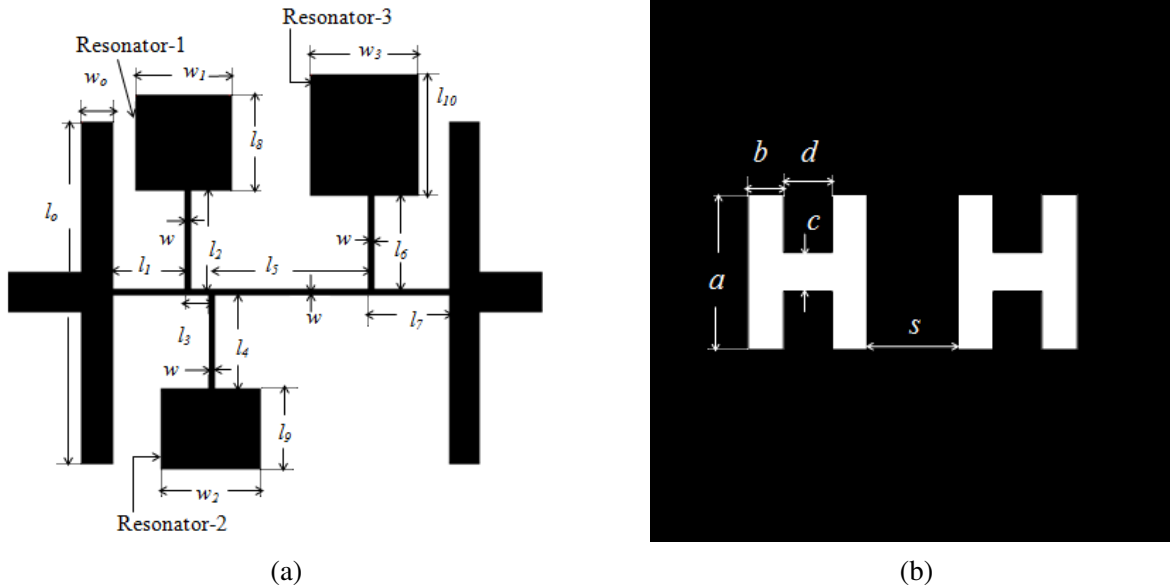


**Figure 5.** Layout of the proposed Filter-1. (a) Top view. (b) Bottom view.

The LC equivalent circuit of Filter-1 is depicted in Figure 6(a). The lumped element values of the basic lowpass filter are calculated using equations in [2]. The values  $L_1$ ,  $L_3$ ,  $L_5$  and  $L_7$  represent the inductance of the main high impedance transmission line of length  $l_1$ ,  $l_3$ ,  $l_5$  and  $l_7$  respectively.  $L_2$ ,  $L_4$  and  $L_6$  are the inductance values.  $C_1$ ,  $C_2$  and  $C_3$  are the capacitance values of Resonators 1, 2 and 3 respectively, and  $C_0$  is the capacitance value of the uniform impedance stub. Component values of equivalent circuit are  $L_1 = 1.941$  nH,  $L_2 = 2.634$  nH,  $L_3 = 0.6239$  nH,  $L_4 = 2.495$  nH,  $L_5 = 4.194$  nH,  $L_6 = 3.4959$  nH,  $L_7 = 2.114$  nH,  $L_H = 0.8089$  nH,  $C_1 = 0.8108$  pF,  $C_2 = 0.69048$  pF,  $C_3 = 1.1275$  pF,  $C_0 = 0.793$  pF,  $C_H = 0.142$  pF, and  $C_p = 0.28$  pF. The proposed Filter-1 is fabricated on an FR4 substrate with the same specifications as mentioned earlier. The physical size of the filter is 15.1 mm  $\times$  14.95 mm. The measurements are carried out on an R & S ZVB 20 Vector Network Analyzer. The measured insertion loss is found to be lower than 0.59 dB up to 1.1 GHz, and return loss in the passband is higher than 21 dB. The cutoff frequency of the filter is 2.02 GHz, and the selectivity obtained is 37.117 dB/GHz at 20 dB suppression level. The stopband bandwidth of Filter-1 at 18 dB suppression level is from 2.45 GHz to 20 GHz. The relative stopband bandwidth of the filter is 156.3%, and the

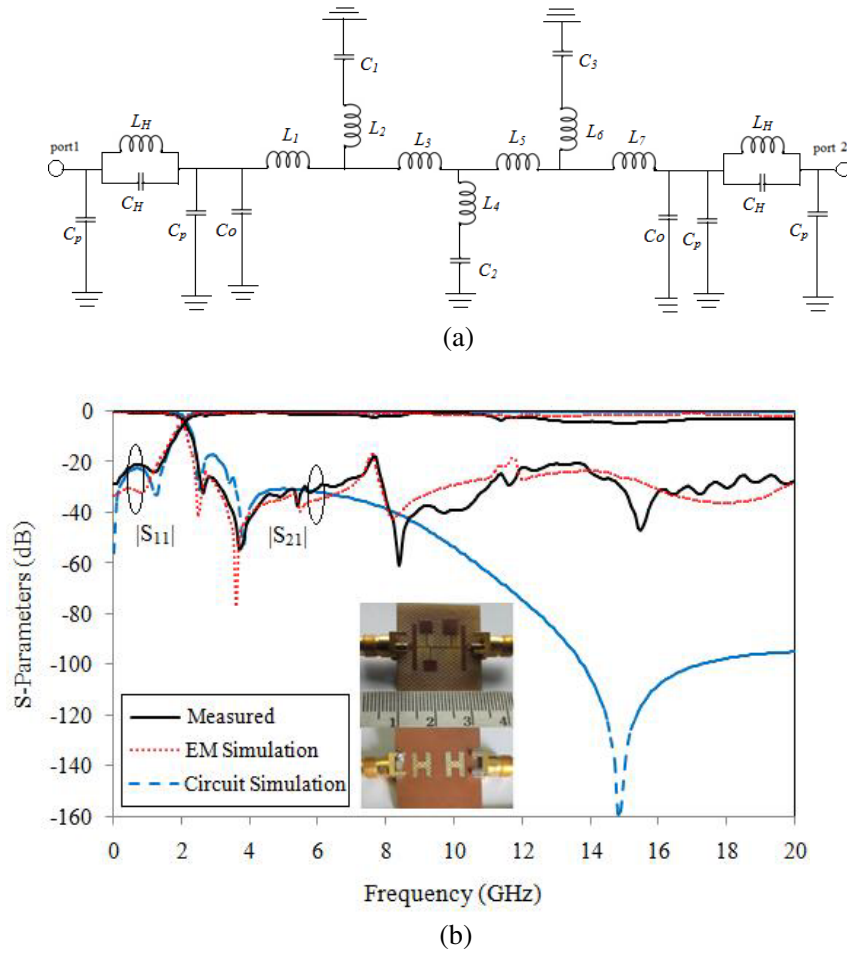


**Figure 6.** (a) LC equivalent circuit of Filter-1. (b) Frequency response of measured, EM and LC circuit simulation of Filter-1.

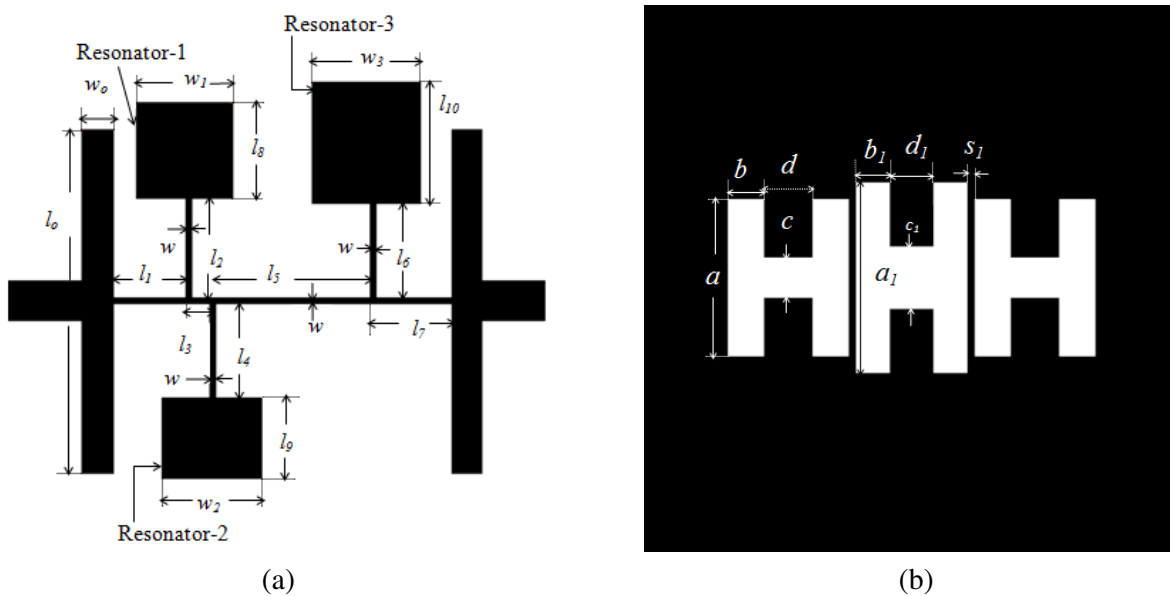


**Figure 7.** The structure of Filter-2. (a) Top view. (b) Bottom view.

normalized circuit size (NCS) is  $0.0338\lambda_g^2$  where  $\lambda_g = 81.61$  mm. Figure 6(b) shows the comparison between measured, EM and LC circuit simulation of Filter-1. It is clear that there is a good agreement between the transmission characteristics of all the results up to 9 GHz, and after that the stopband rejection level of LC circuit simulation result increases rapidly. In the LC equivalent circuit, due to the effect of H-shaped slots in the ground plane, the stopband suppression level increases, and the values of L and C are the only dependent parameters for the analysis of transmission characteristics whereas in EM simulation and measurement results, substrate losses also play a vital role.

To improve the characteristics of Filter-1, one more H-shaped slot is added to the ground plane, and the coupling between the DGS resonators is increased. The new filter, Filter-2, is designed using the same FR4 substrate, which is used in Filter-1. Filter-2 offers improved passband and stopband characteristics as compared to that of Filter-1 without changing its normalized circuit size. Figures 7(a) and 7(b) show the top and bottom views of Filter-2. Due to the addition of one more H-shaped slot of different dimension, the effective permittivity and coupling between DGS resonators are increased. The proposed Filter-2 is designed, fabricated and measured. The dimensions of the newly added H-shaped slot are  $a_1 = 8.6$  mm,  $b_1 = 1.5$  mm,  $c_1 = 2.8$  mm,  $d_1 = 2$  mm and  $s_1 = 0.35$  mm.

## 5. SIMULATION AND MEASUREMENT RESULTS OF FILTER-2

The passband and stopband characteristics of the basic lowpass filter are improved using the DGSs. Due to increased etched area in the ground plane, the simulated 3 dB cutoff frequency of the proposed Filter-2 is reduced to 1.88 GHz. The frequency at 40 dB suppression level is 2.535 GHz, and the selectivity of the filter is 56.48 dB/GHz. The designed Filter-2 has low insertion loss and high return loss values in the passband together with a wide stopband up to 20 GHz at 21 dB suppression level. Figure 8(a) shows the top and bottom photographic views of the fabricated Filter-2. The comparison between measured and simulated results which are in good agreement is shown in Figure 8(b). The measured

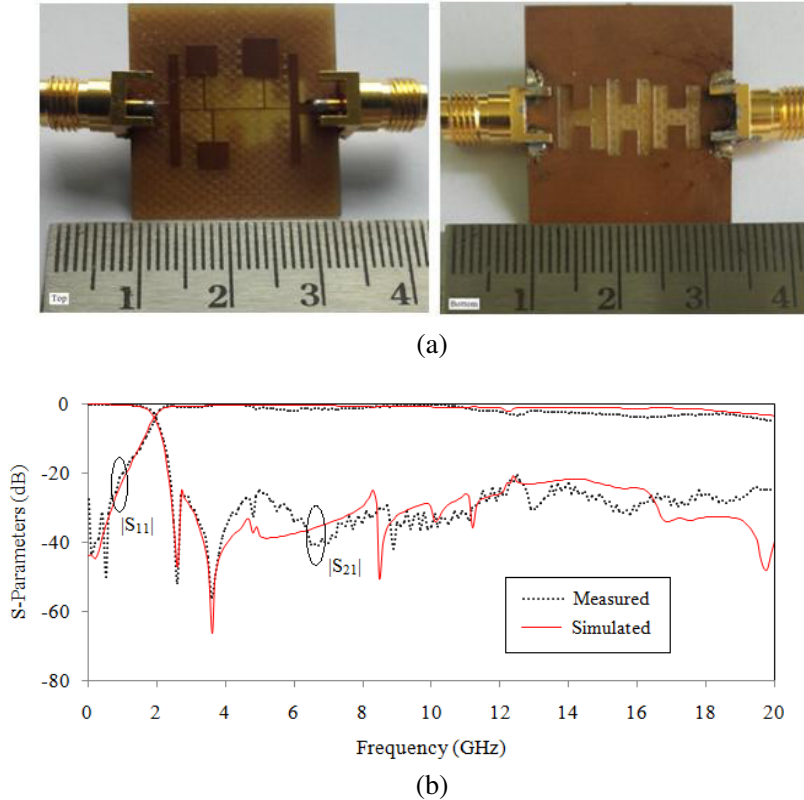


**Figure 8.** (a) Top and bottom view of the Filter-2. (b) Measured and simulated frequency response.

3 dB cutoff frequency of the proposed filter is 1.935 GHz. The transition from passband to stopband frequency at 3 dB and 40 dB is 1.935 GHz to 2.536 GHz; therefore, the selectivity of the proposed filter is 61.56 dB/GHz. The insertion loss in the passband is less than 0.22 dB up to 1.1 GHz, and high return loss of 27 dB is achieved in Filter-2. The stopband bandwidth is from 2.37 GHz to 20 GHz at 20 dB suppression level, and the relative stopband bandwidth achieved is 157.6%. The RSB is increased from 120.1% of the basic lowpass filter to 157.6% by the use of DGSs, and suppression up to 10th harmonics is achieved in Filter-2.

Table 1 shows the performance characteristics of the proposed filters compared with other related works. It is seen that the designed filters have good characteristics such as high return loss in the passband and wide stopband bandwidth at high suppression level. Compared to other works, the proposed filters have compact circuit size.

**Table 1.** Performance comparison of the proposed work with related works.

Ref	CF (GHz)	PB-RL (dB)	SB (GHz @ dB)	RSB%	NCS
[11]	1.8	16	2.8–10 @ 20	112.5	$0.1575\lambda_g^2$
[12]	2.5	18.5	2.58–7.5 @ 20	97.6	$0.0756\lambda_g^2$
[13]	3.37	10	3.46–9.2 @ 20	90.6	$0.036\lambda_g^2$
[14]	3.38	12.5	4.07–15 @ 20	114.6	$0.2016\lambda_g^2$
[15]	1.56	15.7	1.75–20 @ 21	167.8	$0.0673\lambda_g^2$
[16]	2.5	11	2.9–12 @ 20	122.1	$0.0646\lambda_g^2$
<b>Filter-1</b>	<b>2.02</b>	<b>21</b>	<b>2.45–20 @ 18</b>	<b>156.3</b>	<b><math>0.0338\lambda_g^2</math></b>
<b>Filter-2</b>	<b>1.935</b>	<b>27</b>	<b>2.37–20 @ 20</b>	<b>157.6</b>	<b><math>0.0338\lambda_g^2</math></b>

CF — 3 dB Cutoff frequency, PB-RL — Passband return loss, SB — Stopband  
RSB — Relative stopband bandwidth, NCS — Normalized circuit size.

## 6. CONCLUSION

By using a multilayer structure, the performance characteristics of the basic lowpass filter are greatly improved. For validation of the structure, the proposed lowpass filters are fabricated, and their frequency response is analyzed. The designed filter, Filter-2, has very low insertion loss and high return loss in the passband as compared to the performance of the basic filter structure. It also has good selectivity and high rejection in the stopband up to 20 GHz at 20 dB suppression level. Suppression up to the 10th order harmonics is achieved as compared to the basic filter suppressing up to only 5th order. The proposed filter is very compact and offers good performance characteristics in both passband and stopband, thus making it a good choice for mobile and wireless communication applications.

## ACKNOWLEDGMENT

This work was supported in part by Kerala State Council of Science, Technology and Environment, Kerala State, India.

## REFERENCES

1. Pozar, D. M., *Microwave Engineering*, 2nd edition, Wiley, New York, 1998.
2. Hong, J. S. and M. J. Lancaster, *Microstrip Filters for RF/Microwave Applications*, Wiley, New York, 2001.
3. Hsieh, L.-H. and K. Chang, "Compact elliptic-function low-pass filters using microstrip stepped-impedance Hairpin resonators," *IEEE Trans. Microwave Theory Tech.*, Vol. 51, No. 1, 193–199, 2003.

4. Rekha, T. K., P. Abdulla, P. M. Raphika, and P. M. Jasmine, "Compact microstrip lowpass filter with ultra-wide stopband using patch resonators and open stubs," *Progress In Electromagnetics Research C*, Vol. 72, 15–28, 2017.
5. Velidi, V. K. and S. Sanyal, "Sharp roll-off lowpass filter with wide stopband using stub-loaded coupled line Hairpin unit," *IEEE Microwave Wireless Compon. Lett.*, Vol. 21, No. 6, 301–303, 2011.
6. Ahn, D., J.-S. Park, C.-S. Kim, J. Kim, Y. Qian, and T. Itoh, "A design of the low-pass filter using the novel microstrip defected ground structure," *IEEE Trans. Microwave Theory Tech.*, Vol. 49, No. 1, 86–93, 2001.
7. Park, J.-S., J.-H. Kim, J.-H. Lee, S.-H. Kim, and S.-H. Myung, "A novel equivalent circuit and modeling method for defected ground structure and its application to optimization of a DGS lowpass filter," *IEEE MTT-S International Microwave Symposium Digest*, Vol. 1, 417–420, 2002.
8. Abdel-Rahman, A., A. K. Verma, A. Boutejdar, and A. S. Omar, "Control of bandstop response of Hi-Lo microstrip low-pass filter using slot in ground plane," *IEEE Trans. Microwave Theory Tech.*, Vol. 52, No. 31008-1013, 2004.
9. Weng, L. H., Y.-C. Guo, X.-W. Shi, and X.-Q. Chen, "An overview on defected ground structure," *Progress In Electromagnetics Research B*, Vol. 7, 173–189, 2008.
10. Kurgan, P. and M. Kitlinski, "Novel microstrip low-pass filters with fractal defected ground structures," *Microwave Opt. Technol. Lett.*, Vol. 51, No. 10, 2473–2477, 2009.
11. Boutejdar, A. and W. A. Ellatif, "Improvement of compactness of low pass filters using new quasi-Yagi-DGS-resonator and multilayer-technique," *Progress In Electromagnetics Research C*, Vol. 69, 115–124, 2016.
12. Xi, D., Y.-Z. Yin, L.-H. Wen, Y. Mo, and Y. Wang, "A compact low-pass filter with sharp cutoff and low insertion loss characteristic using novel defected ground structure," *Progress In Electromagnetics Research Letters*, Vol. 17, 133–143, 2010.
13. Xiao, M., G. Sun, and X. Li, "A lowpass filter with compact size and sharp roll-off," *IEEE Microwave Wireless Compon. Lett.*, Vol. 25, No. 12, 790–792, 2015.
14. Zhang, P. and M. Li, "A novel sharp roll-off microstrip lowpass filter with improved stopband and compact size using dual-plane structure," *Microwave Opt. Technol. Lett.*, Vol. 58, No. 5, 1085–1088, 2016.
15. Belbachir, A. K., M. Boussouis, and N. Amar Touhami, "High-performance LPF using coupled C-shape DGS and radial stub resonator for microwave mixer," *Progress In Electromagnetics Research Letters*, Vol. 58, 97–103, 2016.
16. Wang, C. J. and T. H. Lin, "A multi-band meandered slotted-ground plane resonator and its application of lowpass filter," *Progress In Electromagnetics Research*, Vol. 120, 249–262, 2011.